# Sensitivity analysis of parameters for probabilistic seismic hazard assessment of western Liguria (north-western Italy)

S. Barani[1], D. Spallarossa[1], C. Eva[1] and P. Bazzurro[2]

[1]*Dipartimento per lo Studio del Territorio e delle sue Risorse, University of Genova, Italy*
[2]*AIR Worldwide Co., San Francisco, CA, USA*

(Received: April 18, 2006; accepted: June 30, 2006)

***ABSTRACT*** In this paper the sensitivity analysis is performed as the preliminary step towards the construction a logic tree useful for probabilistic seismic hazard analyses of western Liguria (north-western Italy). The sensitivity analysis is conducted for six strategic sites within the Imperia district, following a multi-parameter approach, and accounts for both mean hazard values and hazard values corresponding to different percentiles (e.g. 16$^{th}$ and 84$^{th}$ percentile). In this way not only is the effect of a parameter on mean hazard values determined but also its sensitivity for two percentiles. In the analysis presented in this paper, the influence of different seismic catalogues (epicentral parameters), source zone models, frequency-magnitude parameters, maximum earthquake magnitude values and attenuation relationships is considered. As a result, the sensitivity analysis can be used as objective criterion for the construction of a logic tree focusing efforts on the parameters with a greater effect on the hazard. The results, valid just for a medium-low-seismicity and short historical information area such as western Liguria and for a similar set of assumptions in the logic tree, show that the seismic catalogues and the frequency-magnitude parameters have the highest influence on mean PGA values corresponding to a 475-year return period and the 16$^{th}$ percentile while the attenuation relationships have the highest effect on the 84$^{th}$ percentile. Furthermore, we found that the seismogenetic zonations characterized by smaller source zones contribute most to the uncertainty in the hazard.

## 1. Introduction

Probabilistic seismic hazard analysis (PSHA) provides a framework in which it is possible to identify, quantify and combine uncertainties in the size, location and rate of occurrence of earthquakes, seismogenetic source geometry, and in the ground motion as a function of the size and location of earthquakes (Kramer, 1996). In general, distinction is made between two kinds of uncertainty: aleatory and epistemic. The former is related to the randomness of natural phenomena; the latter is due to insufficient knowledge of the input parameters. In PSHA, epistemic uncertainties are incorporated into calculations through the use of logic trees (e.g. Senior Seismic Hazards Analysis Committee, 1997) made of several branches each of which is assigned a weighting factor that represents the relative likelihood of that parameter value and/or model being correct. Hence, the logic tree scheme allows one to consider and quantify the uncertainty in the ground motion that is exceeded with a certain probability (or alternatively, in the probability of exceeding a given ground motion). McGuire and Shedlock (1981), Kulkarni

 

*et al.* (1984), Bender and Perkins (1993), Cramer (1996), Petersen *et al*. (2000), and Cao *et al*. (2005) are examples of uncertainty studies in PSHA.

Since the use of logic trees implies that a seismic hazard analysis is carried out for each combination of models and/or parameters associated with each terminal branch, a long computation time may be required. At present, the use of a very large logic tree is a practical possibility. Therefore, the major disadvantage in performing logic tree analyses is not computational but analytical, and is represented by the time that researchers have to spend to determine what values of each input parameter should be included in the tree and what probabilities should be assigned to them. Therefore, the sensitivity analysis is useful in preparing logic trees focusing efforts on the parameters that have greater impact on seismic hazard, and may help in reducing both the calculation time and above all the analyst time (Rabinowitz *et al*., 1998).

The potential of the sensitivity analysis is used in this paper in order to identify the parameters that have the largest influence on the western Liguria (north-western Italy) seismic hazard. Western Liguria is characterized by moderate-to-strong seismicity, both distributed in well defined onshore areas and along the main active faults in the Ligurian Sea (Eva *et al.*, 1999). The historical seismicity shows that strong earthquakes have occurred in the past [February 23, 1818, $I_0$ = VII-VIII; January 8, 1819, $I_0$ = VI - VII; May 26, 1831, $I_0$ = VIII; December 29, 1854, $I_0$ = VII-VIII; February 23, 1887, $I_0$ = IX; $I_0$ indicates the Mercalli-Cancani-Sieberg (MCS) epicentral intensity] but their epicentral positions are strongly uncertain. In fact, some of them might have been generated by offshore faults rather than inland (e.g. Ferrari, 1991; Eva and Rabinovich, 1997; Pelinovsky *et al*., 2001, 2002; Tinti *et al*., 2004).

The sensitivity analysis is performed following the multi-parameter approach originally proposed by Rabinowitz and Steinberg (1991), and applied by several authors (e.g. Rabinowitz *et al.*, 1998; Giner *et al*., 2002a, 2002b). This approach is applied instead of the one-parameter-at-a-time method (e.g. Atkinson and Charlwood, 1983; Cramer, 1996; Grünthal and Wahlström, 2001) which consists of examining, in turn, the sensitivity of each input parameter while holding the others at their default levels. The multi-parameter approach, instead, consists of assessing the effect of each input parameter at different settings of the other parameters and consequently it allows one to identify whether the effect of a parameter on the hazard depends on the settings of the remaining parameters. In this study, the sensitivity analysis enables us to investigate the influence of individual parameters of a preliminary logic tree (Fig. 1) that allows uncertainty in selection of epicentral parameters (latitude, longitude and magnitude), source zone models, several values of earthquake recurrence parameters, maximum earthquake magnitude (interpreted as the upper bound of magnitude for a given seismogenetic zone) and different rock-ground motion predictive attenuation relationships. Following the paths of this logic tree, the number of the marginal branches is 144. In the application presented here, all the branches of a node have the same weight. We evaluate the effect of parameters on both the mean horizontal peak ground acceleration (*PGA*) with a 10% probability of exceedance in 50 years (mean return period, MRP, of 475 years) and two different percentiles (e.g. $16^{th}$ and $84^{th}$ percentile, hereinafter 16%-ile and 84%-ile).

As a result, the sensitivity analysis allows us to identify the parameters with little or no effect on the hazard. These parameters can be excluded from subsequent logic tree analyses while those with substantial influence should be subjected to careful discussion and/or further studies in order

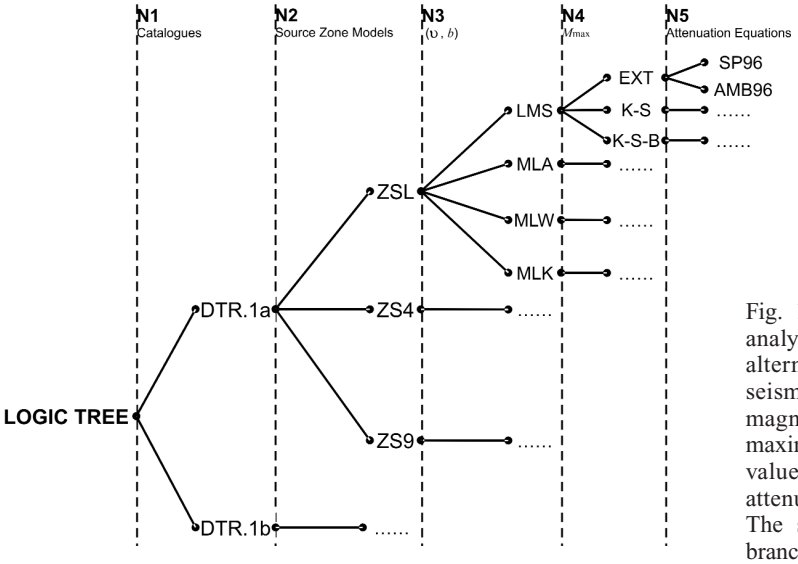


Fig. 1 - Logic tree for the sensitivity analysis. Nodes N1 to N5 refer to alternative earthquake catalogues, seismogenetic zonations, frequency-magnitude parameter ($\upsilon$, $b$) values, maximum earthquake magnitude ($M_{max}$) values, and rock-ground motion attenuation relationships respectively. The same weight is given to all the branches of each node.

to reduce the uncertainty in the hazard.

## 2. Earthquake data

In this study, two databases, called DTR.1a and DTR.1b (Dip.Te.Ris. parametric seismic catalogue of earthquakes in northern Italy - version "1a" and "1b"; Dip.Te.Ris. indicates "Dipartimento per lo Studio del Territorio e delle sue Risorse"), are compiled to account for the uncertainty in the epicentral location of the main earthquakes that occurred in western Liguria. Both the catalogues collect historical and instrumental data (e.g. time and location of earthquakes, magnitude, etc.) and differ from one another in the epicentral parameters of four earthquakes which occurred in 1818, 1819, 1854 and 1887 (see Table 1). The historical earthquakes, from year 1000 to 1980, are obtained from the CPTI04 catalogue (Gruppo di lavoro CPTI, 2004) that was used for the evaluation of the Italian seismic hazard map (Gruppo di lavoro MPS, 2004a). The instrumental data, from year 1981 to 2003, are selected from two databases: the CSTI catalogue (Augliera *et al*., 1998) that holds all the Italian earthquakes from 1981 to 1996 and the bulletin of the RSNI seismic network (Regional Seismic Network of north-western Italy; University of Genoa) for the period going from 1997 to 2003. All the instrumental earthquakes with magnitude $M_l \geq 3.2$, azimuthal distance between the nearest seismic stations GAP ≤ 210°, minimum distance from the nearest station ≤ 200 km, number of phase picks ≥ 8, and root mean square value of travel time residuals RMS ≤ 3.0 are considered. Homogeneous magnitude values are then assigned to each event. Two types of magnitude are considered: $M_s$ and $M_{sp}$. The former is the surface wave magnitude. The latter is estimated for the application of the Sabetta and Pugliese (1996) attenuation model and coincides with $M_l$ for $M_s < 5.5$ and with $M_s$ for $M_s \geq 5.5$. The instrumental magnitude $M_l$ is converted to $M_s$ using the conversion equation proposed for the CPTI04 catalogue (Gruppo di lavoro MPS, 2004b):

Table 1 - Epicentral parameters of the 1818, 1819, 1854, 1887 earthquakes. Epicentral position, epicentral intensity $I_0$ according to the MCS scale, and magnitude $M_s$ and $M_{sp}$ are listed.

| Date | Long - Lat *(DTR.1a)* | Long - Lat *(DTR.1b)* | $I_0$ | $M_s$ | $M_{sp}$ |
|---|---|---|---|---|---|
| February 23, 1818 | 8.130 - 43.740 | 8.034 - 43.920 | VII - VII | 5.37 | 5.52 |
| Jabuary 8, 1819 | 8.060 - 43.710 | 8.200 - 44.050 | VI - VII | 4.70 | 4.90 |
| December 29, 1854 | 7.730 - 43.630 | 7.550 - 43.820 | VII - VIII | 5.69 | 5.69 |
| February 23, 1887 | 8.130 - 43.740 | 8.070 - 43.920 | IX | 6.29 | 6.29 |

$$M_s = 1.079\, M_l - 0.584 \qquad (3.0 < M_l < 7.5,\ \sigma_M = 0.40) \tag{1}$$

As mentioned before, DTR.1a and DTR.1b differ from one another in the epicentral parameters of four historical earthquakes that are listed in Table 1. In particular, DTR.1b accounts for the CPTI04 epicentral data while DTR.1a includes offshore localizations of the 1818, 1819, 1854 and 1887 earthquakes. The offshore epicentres are determined in this study after analysing the distribution of the recent seismicity (Fig. 2), the seismotectonic background, and the macroseismic fields (Fig. 3) [DOM4.1 database, Monachesi and Stucchi, (2000)]. For all the earthquakes mentioned above, the distribution of the macroseismic intensities felt onshore shows a general progression of the macroseismic fields towards the Ligurian Sea, which implies a distribution of the maximum seismic effects along the sea coast. Then, it must be considered that the 1818, 1854, and 1887 earthquakes caused tsunami waves as indicated by several authors (Eva and Rabinovich, 1997; Pelinovsky *et al*., 2001, 2002; Tinti *et al*., 2004).

Following the previous observations, an alternative epicentral position is proposed for the 1818, 1819, 1854 and 1887 earthquakes. All the epicentres are localized at 15 to 20 km offshore from the coast at the base of the continental slope on NE-SW faults (oriented parallel to the extension of the iso-felt areas, see Fig. 4) where the seismicity is mainly concentred (Augliera *et al*., 1994; Eva *et al*., 2001) (Fig. 2). The 1818 and the 1819 events are localized in the area of the 1887 earthquake while that of 1854 is set further west on the fault system that caused the December 26, 1989 earthquake ($M_l$ = 4.2) and the April 15, 1990 earthquake ($M_l$ = 3.9).

The epicentral intensity of the four re-localized earthquakes is estimated using a trial and error procedure that simulates the macroseismic fields by the attenuation of intensities proposed by Grandori *et al*. (1991):

$$I_0 - I_i = \frac{1}{\ln \psi} \ln\left[1 + \frac{\psi - 1}{\psi_0}\left(\frac{D_i}{D_0} - 1\right)\right], \tag{2}$$

where $I_0$ is the epicentral intensity, $I_i$ the intensity of the $i_{th}$ isoline, $D_i$ the epicentral distance of the $i_{th}$ intensity class, $D_0$ the radius of the zero-decay isoline and $\psi$ and $\psi_0$ are regression coefficients. For the Ligurian Sea $D_0$ = 3.48, $\psi$ = 1.45 and $\psi_0$ = 2.59 (Peruzza, 1996).

After a visual inspection, the best agreement between the macroseismic fields from the

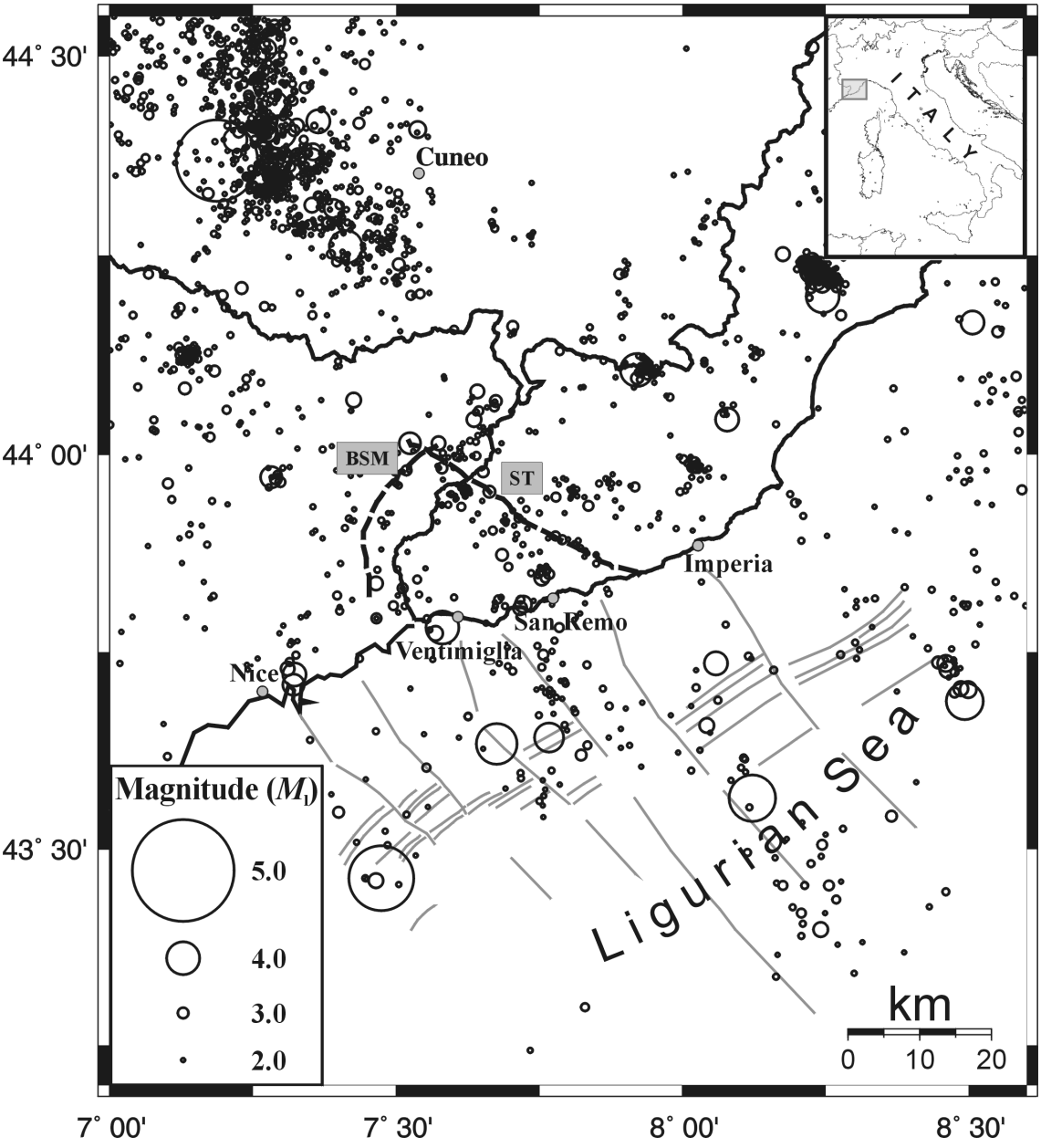


Fig. 2 - Map of the instrumental seismicity. The earthquakes from year 1981 to 2003 with $M_l \geq 2.0$ are shown.

DOM4.1 database and the calculated isoseismal lines is obtained for $I_0$ values equal to those provided by the CPTI04 catalogue with the exception of the 1819 earthquake whose calculated $I_0$ = VI-VII is the same as that of the DOM4.1 database (Monachesi and Stucchi, 2000). Once the epicentral intensities have been calculated, the $M_s$ magnitude is estimated using the intensity-magnitude conversion table as in CPTI04 (Gruppo di lavoro MPS, 2004b). Fig. 4

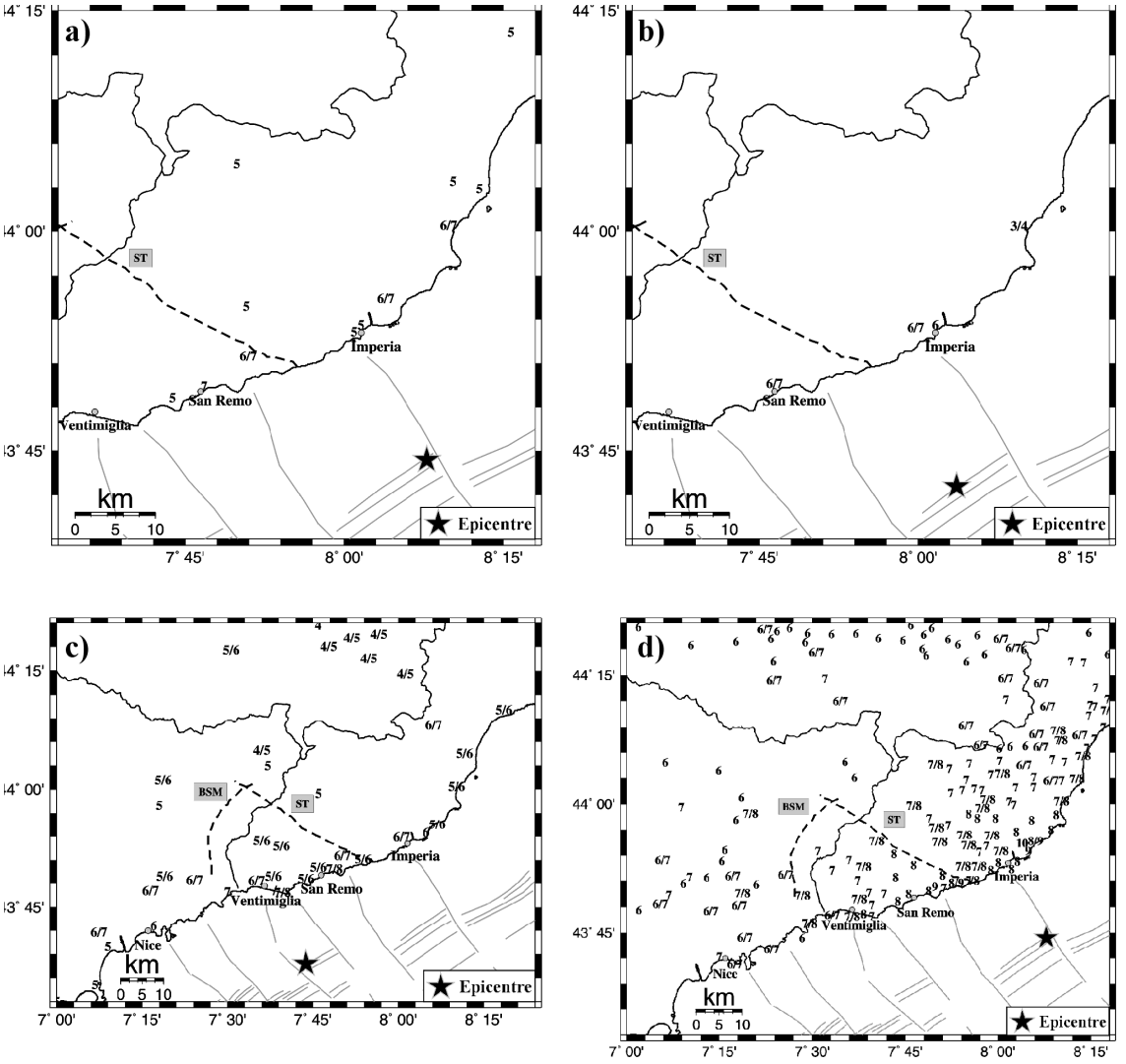


Fig. 3 - Macroseismic fields of the 1818 (a), 1819 (b), 1854 (c) and 1887 (d) earthquakes. Not all the points of the macroseismic fields of the 1854 and 1887 earthquakes are marked, but only a selection of the most significant ones. Intensities are assigned according to the MCS scale.

shows the seismicity distribution from year 1000 to 2003 accounting for both the onshore (DTR.1b) and offshore (DTR.1a) epicentral localizations.

## 3. Seismogenetic zonations

The preliminary logic tree considers three source zone models (Fig. 5), ZS4 (Meletti *et al.*, 2000), ZSL, and ZS9 (Gruppo di lavoro MPS, 2004c), that represent different interpretations of the seismicity, seismotectonic background, and structural geology.

The ZSL zonation has been properly developed for seismic hazard analyses of western

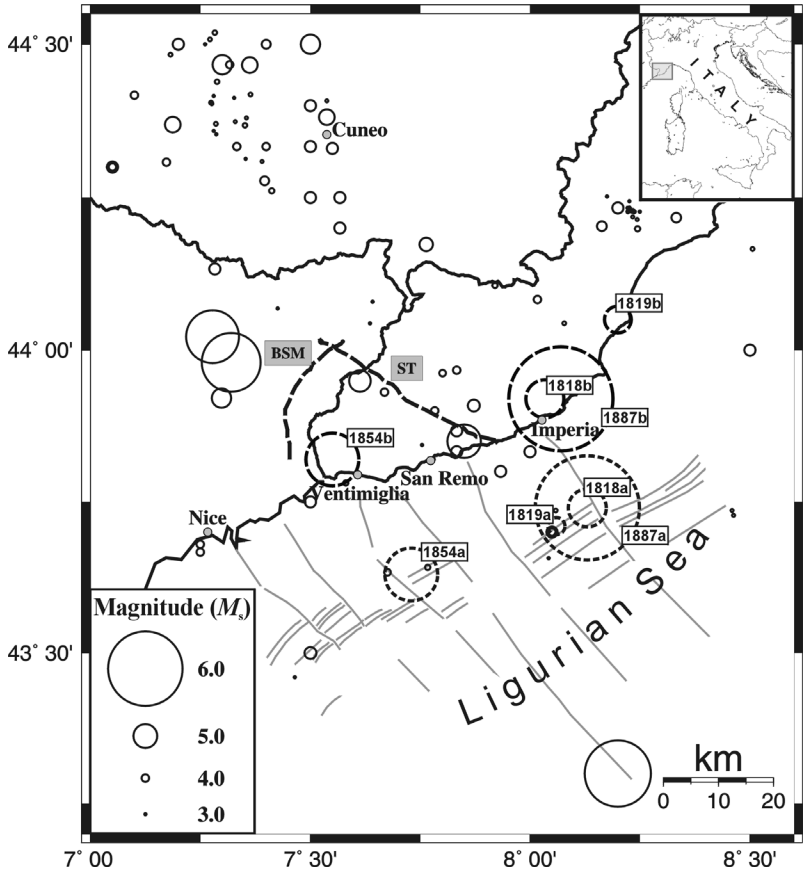


Fig. 4 - Ligurian seismicity from year 1000 to 2003. The 1818, 1819, 1854, 1887 offshore (DTR.1a) and onshore (DTR.1b) epicentres are shown by dotted circles and white labels (e.g. 1818a for DTR.1a, 1818b for DTR.1b).

Liguria. It derives from ZS4 and results from the correlation between the seismicity distribution, seismotectonic patterns, geodynamics, neotectonics, and geophysics (e.g. Béthoux *et al*., 1992; Chaumillon *et al*., 1994; Eva and Solarino, 1998; Contrucci *et al*., 2001). Each source zone (SZ) consists of all the active faults and seismotectonic units that characterize an area which is supposed to be homogeneous with respect to the seismic activity. The SZ 94, 96 and 97 (see Fig. 5b) enclose the offshore seismicity that is mainly associated with the fault system that characterizes the foot of the continental slope. It is worth noting that the offshore seismic activity is not continuous but is characterized by a lack of seismicity (see Figs. 2 and 4) that seems to be almost coincident with a high heat-flux zone outlined by Pasquale *et al*. (1994, 1996). The kinematic behaviour of these zones is associated with a compression (thrust and left-lateral strike-slip) overprinting a previous extensional regime (Béthoux *et al*., 1992; Eva and Solarino, 1998). The Ligurian seismicity is mainly concentrated in the SZ 96 and 97 (Fig. 5b) which consist of all the seismic sources characterizing the centre of the Ligurian Sea basin and the continental slope respectively. Both source zones have been affected in the past by strong earthquakes: the strongest ones were the July 19, 1963 ($M_s$ = 5.9) and February 23, 1887 ($M_s$ = 6.3) earthquakes.

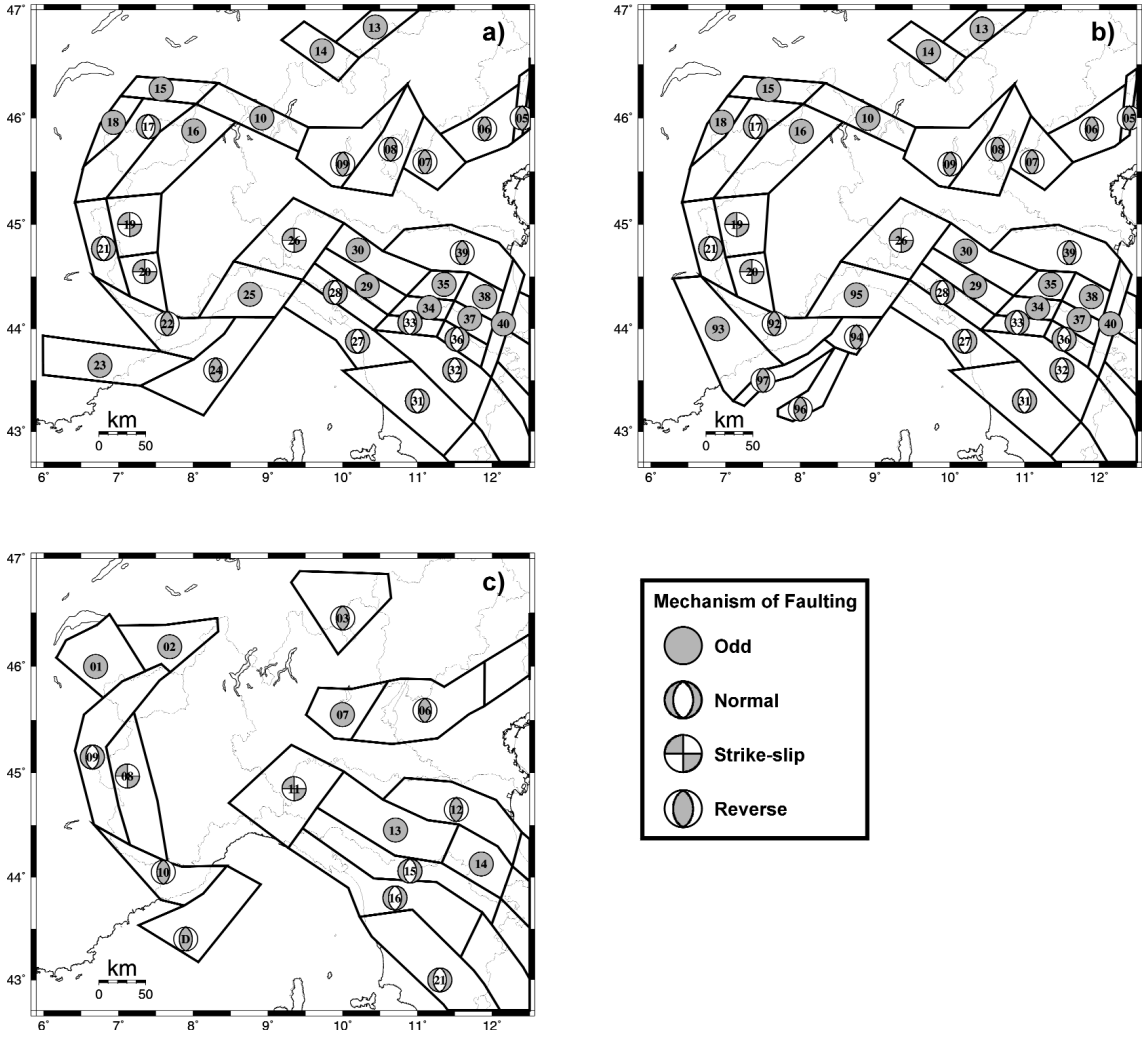


Fig. 5 - Seismogenic zonations: ZS4 (a); ZSL (b); ZS9 (c). The prevalent mechanism of faulting of each source zone is marked by a beach ball.

The SZ 94 (Fig. 5b) includes the modest seismicity localized in front of the harbour of Savona. The SZ 92 and 93 (Fig. 5b) outline the weak seismic activity of the continental platform, the onshore seismicity and the seismotectonic sources that characterize western Liguria, the Piedmont region and eastern France. The onshore seismicity is mainly associated with the Saorge-Taggia (ST) and the Breil-Sospel-Monaco (BSM) fault systems (see Figs. 2 and 4). Reverse and left-lateral strike-slip mechanisms prevail in the SZ 92 (Fig. 5b) while the SZ 93 (Fig. 5b) is characterized by different styles of deformation: normal faulting in the north-eastern part, left-lateral strike-slip mechanisms in shallower crustal structures and dip-slip mechanisms in deeper crustal structures (Eva and Solarino, 1998; Meletti *et al.*, 2000). The SZ 95 (Fig. 5b) is just a revision of the corresponding SZ 25 (ZS4 source zone model, Fig. 5a) due to the geometry of the neighbouring source zone regions.

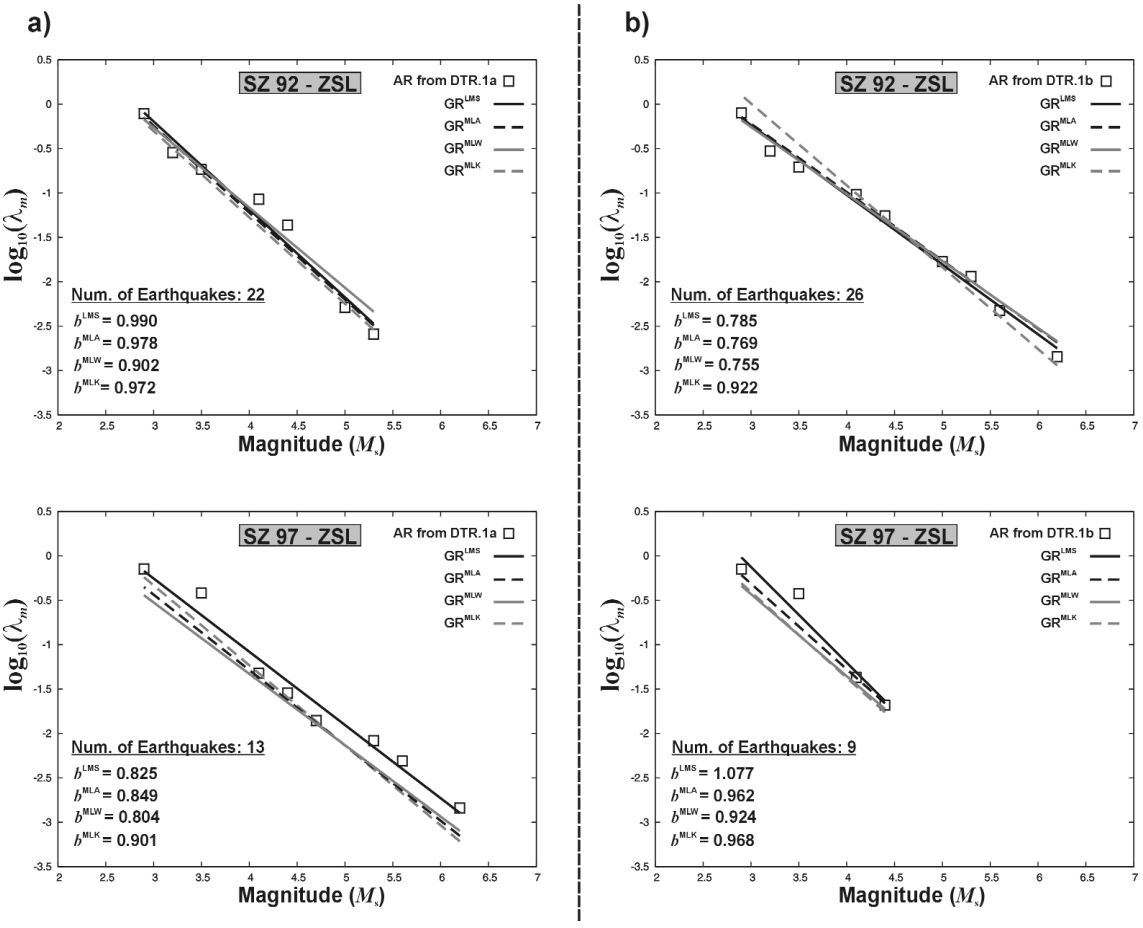


Fig. 6 - Gutenberg-Richter (GR) distributions and values of the parameter *b* obtained by applying the LMS, MLA, MLW, and MLK procedures (indicated by superscript) for the SZ 92 and the SZ 97 of the ZSL seismogenetic zonation (Fig. 5b). Observed activity rates (AR) in Fig. 6a and Fig. 6b are based on the DTR.1a and DTR.1b catalogues respectively.

Originally, only ZS9 assigned a prevalent mechanism of faulting (interpreted as the mechanism with the highest probability of generating future earthquakes) to all its source zones. According to Sadigh *et al*. (1997), mechanisms have been classified in three categories on the basis of the rake angle, $\gamma$: normal ($-135° \leq \gamma \leq -45°$), reverse ($45° \leq \gamma \leq 135°$) and strike-slip ($|\gamma| < 45°$ or $\gamma < -135°$ or $\gamma > 135°$). A mechanism has been classified as odd when the data are not sufficient to unambiguously define a prevalent style-of-faulting. In this study, a prevalent mechanism is assigned to all the source zones of ZS4 and ZSL in order to consider the style of faulting into equations to predict ground motions. Following the same classification criteria that have been adopted in ZS9, mechanisms are assigned to ZS4 and ZSL using several data (e.g. Eva and Solarino, 1998; Meletti *et al*., 2000; Vannucci and Gasperini, 2004; Vannucci *et al*., 2004) and by a simple superposition of ZS4 and ZSL on ZS9 since a lot of zones of ZS9 derive from uniting the ZS4 ones (Gruppo di Lavoro MPS, 2004c).

## 4. Frequency-magnitude parameters and maximum earthquake magnitude

In this study, different sets of seismicity parameters (annual rate of earthquake occurrence above a minimum threshold magnitude, $\upsilon$; negative slope of the Gutenberg-Richter (hereinafter GR) relation, $b$; maximum earthquake magnitude, $M_{\max}$) are computed for each source zone. Those zones, characterized by too small a number of earthquakes (e.g. less than eight events), are not considered in the hazard calculation (e.g. SZ 10 of either the ZS4 and ZSL seismogenic zonations) or, as suggested for the evaluation of the Italian seismic hazard map (Gruppo di lavoro MPS, 2004a), account for the values of the parameters ($\upsilon$, $b$) of neighbouring seismically-consistent source zones which include a greater number of events, statistically sufficient to obtain seismicity rates (e.g. the SZ 94 of the ZSL zonation accounts for the parameters evaluated for the SZ 95).

The branches at the third and fourth node of the preliminary logic tree (Fig. 1) represent the multiple choices of the frequency-magnitude parameters ($\upsilon$, $b$) and the maximum earthquake magnitude, respectively.

We considered four branches that correspond to four different procedures to calculate the values of the parameters ($\upsilon$, $b$): Least Mean Square (LMS); Aki maximum likelihood [MLA: Aki, (1965)]; Weichert maximum likelihood [MLW: Weichert (1980)]; Kijko maximum likelihood [MLK: Kijko and Sellevoll, (1989, 1992)]. It is worth noting that the MLK approach allows the use of all available seismicity information from an earthquake catalogue containing both incomplete historical observations and more complete instrumental data [for details see Kijko and Sellevoll, (1989, 1992)].

A comparison between the GR distributions resulting from the application of the previously mentioned procedures is illustrated in Fig. 6 for two source zones, one inland (SZ 92) and one offshore (SZ 97), of the ZSL seismogenic zonation (Fig. 5b). The base-10 logarithm of the number of earthquakes with magnitude equal to or greater than $m$ per year (mean annual rate of exceedance of an earthquake of magnitude $m$), $\lambda_m$, is plotted against magnitude. For each source zone, the number of earthquakes, the activity rates (cumulative number of earthquakes centred on magnitude $m$ divided by the time period of observation; hereinafter AR) observed from the catalogues DTR.1a (Fig. 6a) and DTR.1b (Fig. 6b), and the $b$-values are also indicated. As shown in Fig. 6, and for most of the source zones considered in this study, the MLK procedure tends to overestimate the slope, $b$, of the GR relation and underestimate the number of large magnitude earthquakes (e.g. $m > 4.5 – 5.0$). Hence, the values of the frequency-magnitude parameters from MLK should decrease the hazard. Furthermore, Fig. 6 allows us to evaluate the influence of the DTR.1a and DTR.1b catalogues on the GR distributions relevant at the SZ 92 and the SZ 97 (Fig. 5b). As expected, the $b$-values resulting from DTR.1a for the SZ 92 are higher than those obtained for the SZ 97 (Fig. 6a). On the contrary, $b$-values based on DTR.1b are lower inland than offshore (Fig. 6b).

Three approaches are used to estimate the value of the maximum earthquake magnitude, which is interpreted here as the upper bound value for each seismogenic zone. The first, called EXT, provides a sharp cut-off maximum magnitude by an iterative procedure based on the extrapolation of the standard log-linear GR relation. The frequency-magnitude curve is truncated at the mean annual rate of occurrence corresponding to a maximum magnitude value, $M_{max}$ that gives the best eye-fit of the observed activity rates assuming that magnitudes are

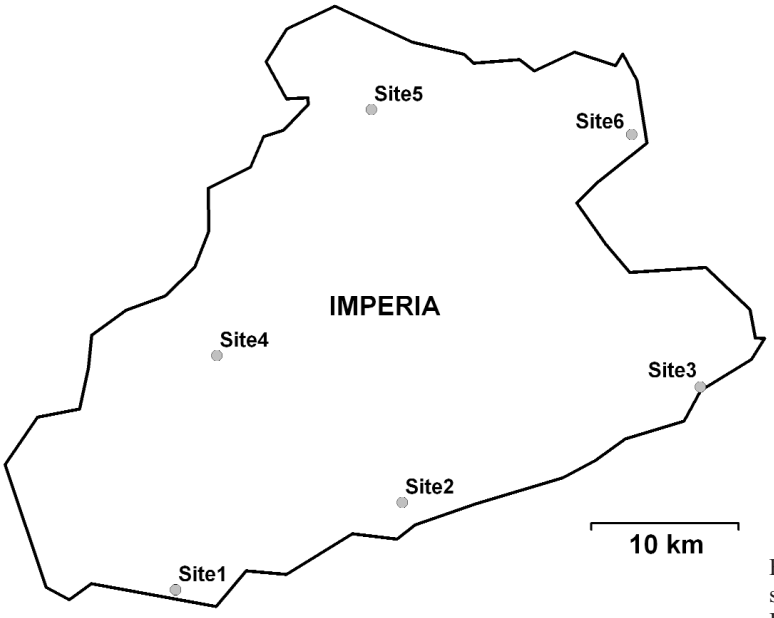


Fig. 7 - Test sites selected for the sensitivity analysis within the Imperia district.

random values following a doubly-truncated exponential distribution (McGuire and Arabasz, 1990):

$$\lambda_m = \upsilon \frac{e^{\left[-\beta(m-m_0)\right]} - e^{\left[-\beta(M_{\max}-m_0)\right]}}{1-e^{\left[-\beta(M_{\max}-m_0)\right]}} \qquad m_0 \le m \le \boldsymbol{M}_{\max} \tag{3}$$

where $\lambda_m$ is the mean annual rate of exceedance of an earthquake of magnitude $m$, $m_0$ is the lower bound magnitude considered for each source zone, $\upsilon = \exp(\alpha - \beta m_0)$ and $\alpha = a \cdot \ln(10)$ and $\beta = b \cdot \ln(10)$ are the GR coefficients obtained with the previously mentioned methodologies.

The other two procedures applied here use the Kijko and Sellevoll estimator (K-S) and the Bayesian Kijko and Sellevoll estimator [K-S-B: Kijko and Graham (1998), Kijko (2004)]. Both methodologies are based on the same generic equation that includes case (1), when earthquake magnitudes follow the doubly-truncated GR relation (K-S estimator), and case (2) when the variation of seismic activity is considered a random process (K-S-B estimator).

Table 2 shows a comparison between the values of the maximum earthquake magnitude resulting from the application of the K-S $\left(M_{\max}^{\text{K-S}}\right)$, K-S-B $\left(M_{\max}^{\text{K-S-B}}\right)$, and EXT $\left(M_{\max}^{\text{EXT}}\right)$ procedures for each SZ of the ZS9 seismogenetic zonation (Fig. 5c). The table shows that both the Kijko and Sellevoll estimators, particularly K-S-B, provide values of $M_{\max}$ that are closer to those of the maximum observed magnitude, $M_{\max}^{obs}$. The EXT solutions, instead, are more conservative since they generally overestimate the $M_{\max}^{obs}$ values more than those provided by K-S and K-S-B.

Table 2 - Maximum earthquake magnitude values resulting from the application of the K-S ($M_{max}^{K\text{-}S}$), K-S-B ($M_{max}^{K\text{-}S\text{-}B}$), and EXT ($M_{max}^{EXT}$) procedures for each source zone (SZ) of the ZS9 seismogenetic zonation (Fig. 5c). ($M_{max}^{K\text{-}S}$), ($M_{max}^{K\text{-}S\text{-}B}$), and ($M_{max}^{EXT}$) are estimated accountug for the values of the parameters ($\upsilon$, $b$) which are based on the DTR.1a catalogue and result from the application of the Kijko and Sellevoll procedure (MLK). The values of the maximum observed magnitude ($M_{max}^{obs}$) from DTR.1a are also listed. All the magnitude values refer to the $M_S$ magnitude scale.

| SZ | $M_{max}^{OBS}$ | $M_{max}^{K\text{-}S}$ | $M_{max}^{K\text{-}S\text{-}B}$ | $M_{max}^{EXT}$ |
|---|---|---|---|---|
| 01 | 5.73 | 6.02 | 5.97 | 6.20 |
| 02 | 6.10 | 6.69 | 6.57 | 6.70 |
| 03 | 5.72 | 6.10 | 6.01 | 6.20 |
| 06 | 6.49 | 7.00 | 6.97 | 7.10 |
| 07 | 5.54 | 5.73 | 5.72 | 6.20 |
| 08 | 5.55 | 6.22 | 6.10 | 6.20 |
| 09 | 5.35 | 5.47 | 5.46 | 5.70 |
| 10 | 5.85 | 6.38 | 6.30 | 6.30 |
| 11 | 5.55 | 6.03 | 5.96 | 6.20 |
| 12 | 5.85 | 6.09 | 6.03 | 6.40 |
| 13 | 5.82 | 5.86 | 5.86 | 6.30 |
| 14 | 5.99 | 6.73 | 6.58 | 6.70 |
| 15 | 6.48 | 6.78 | 6.69 | 7.10 |
| 16 | 5.32 | 5.78 | 5.62 | 5.80 |
| 21 | 5.90 | 6.35 | 6.17 | 6.50 |
| D | 6,29 | 7.04 | 6.95 | 7.00 |

## 5. Ground motion prediction equations

In this study, we predict the horizontal (PGA) for rock conditions using two attenuation equations.

Ambraseys *et al*. (1996; hereinafter AMB96). This is derived from a database that collects European and south-western Asia earthquakes (it includes some Italian earthquakes: Friuli 1976; Valnerina 1979, Irpinia 1980, Gubbio 1984):

$$\log_{10}(PGA) = -1.48 + 0.266\, M_s - 0.922 \log_{10}(d^2 + 3.52^2)^{0.5};\ \ \sigma = 0.25 \qquad (4)$$

where $M_s$ is the surface wave magnitude, $d$ is the shortest distance from the station to the surface projection of the fault rupture (km), and $\sigma$ is the standard deviation of the $\log_{10}$ (*PGA*).

Sabetta and Pugliese (1996; hereinafter SP96). This is calibrated using Italian data:

$$\log_{10}(PGA) = -1.845 + 0.363\, M_{sp} - 1.0 \log_{10}(r^2 + 5.0^2)^{0.5};\ \ \sigma = 0.190 \qquad (5)$$

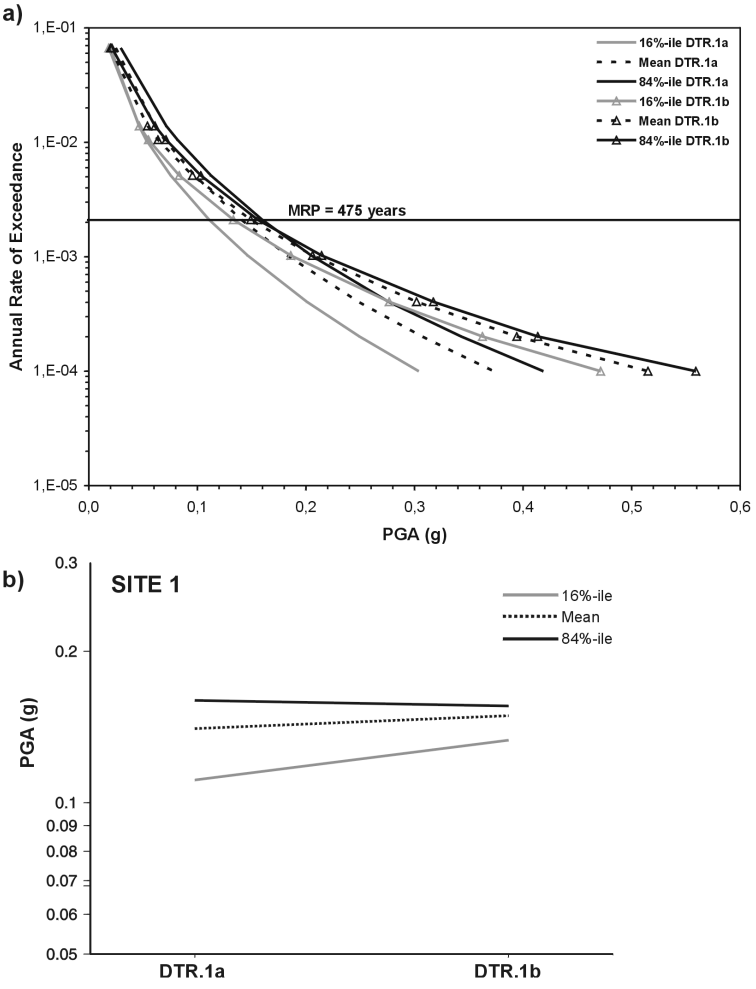


Fig. 8 - Seismic hazard curves calculated from the combination of models and parameters associated with Branch DTR.1a and Branch DTR.1b at Site 1 (a), and *PGA* values corresponding to a MRP of 475 years for each alternative branch (b).

where $M_{sp}$ coincides with $M_l$ for $M_s < 5.5$ and with $M_s$ for $M_s \geq 5.5$, $r$ is the epicentral distance (km), and $\sigma$ is the standard deviation of the $\log_{10}$ (*PGA*).

Since an empirical regression relationship is adopted for the conversion between two magnitude scales ($M_l$ and $M_s$), the $\sigma$ of the ground motion prediction equations has to account for the effect of the error propagation (due to the conversion) by using the expression (Bommer *et al*., 2005):

$$\sigma_{tot} \sqrt{\sigma^2 \left( \frac{\partial \log_{10}(PGA)}{\partial M} \right)^2 \sigma_M^2} \qquad (6)$$

where $\sigma_M = 0.40$ and $\sigma$ is the standard deviation of the $\log_{10}(PGA)$. As a consequence, the $\sigma$ values for the AMB96 and the SP96 relationships increase to 0.272 and 0.239 respectively.

Table 3 - Probabilities $P_{mech}$ associated with the distribution of focal mechanisms in the data sets used to derive the attenuation equations AMB96 and SP96, and adjustment factors $F_{mech:eq}$ for normal (*n*), strike-slip (*ss*), and reverse (*r*) mechanisms.

| Attenuation Equation | $P_n$ | $P_r$ | $F_{n:eq}$ | $F_{ss:eq}$ | $F_{r:eq}$ |
|---|---|---|---|---|---|
| **AMB96** | 0.3069 | 0.4455 | 0,88 | 0.93 | 1.13 |
| **SP96** | 0.4988 | 0.4410 | 0.89 | 0.94 | 1.15 |

Originally, both the attenuation relationships mentioned above did not include the fault mechanism. Bommer *et al*. (2003) developed a methodology that allows the introduction of style-of-faulting into ground motion prediction equations that do not include this parameter. The method is based on the statistical distribution of records used to derive an equation with respect to three mechanisms of faulting groups (normal, reverse, and strike-slip) and the conservative assumption that the aleatory variability of the data within each category is equal to the overall aleatory uncertainty of the data. Equation-specific estimates of adjustment multiplicative factors, $F_{mech:eq}$, are assessed as follows:

$$F_{mech:eq} = F_{eq:ss}^{-1} \cdot F_{mech:ss} \tag{7}$$

where $F_{eq:ss} = F_{r:ss}^{P_R} \cdot F_{n:ss}^{P_n}$ is the factor representing the average behaviour of the predictive equation with respect to the strike-slip condition, $F_{r:ss}$ and $F_{n:ss}$ indicate the factors corresponding to the ratio of the ground motion for reverse and normal mechanisms over the ground motion for strike-slip mechanism respectively, and $P_r$ and $P_n$ are the probability that a record randomly chosen in the dataset used to derive attenuation equations will correspond to a reverse and a normal mechanism respectively.

Bommer *et al*. (2003) proposed an upper, average and a lower value for $F_{r:ss}$ and $F_{n:ss}$. In this study only the average values, $F_{r:ss}$ = 1.22, $F_{n:ss}$ = 0.95, are considered as for the evaluation of the Italian seismic hazard map (Gruppo di lavoro MPS, 2004a) and in Montaldo *et al*. (2005). The values of $P_r$ and $P_n$ assumed here are those tabulated in Bommer *et al*. (2003) using the method proposed by Sadigh *et al*. (1997) for the classification of records in each one of the three style-of-faulting categories. Table 3 lists the coefficient $P_r$ and $P_n$, and the adjustment factors applied to the equations SP96 and AMB96.

## 6. Methodology

The multi-parameter sensitivity analysis (Rabinowitz and Steinberg, 1991) is based on the statistical theory of factorial designs stating that experiments will be more informative if many parameters are varied simultaneously rather than one at a time. This procedure consists of relating the ground motion that is exceeded with a certain probability (or alternatively, the annual rate of exceedance of a certain level of ground motion) to each branch of a logic tree by simultaneously varying all input parameters. The effect of a node of a logic tree is defined as the range in the

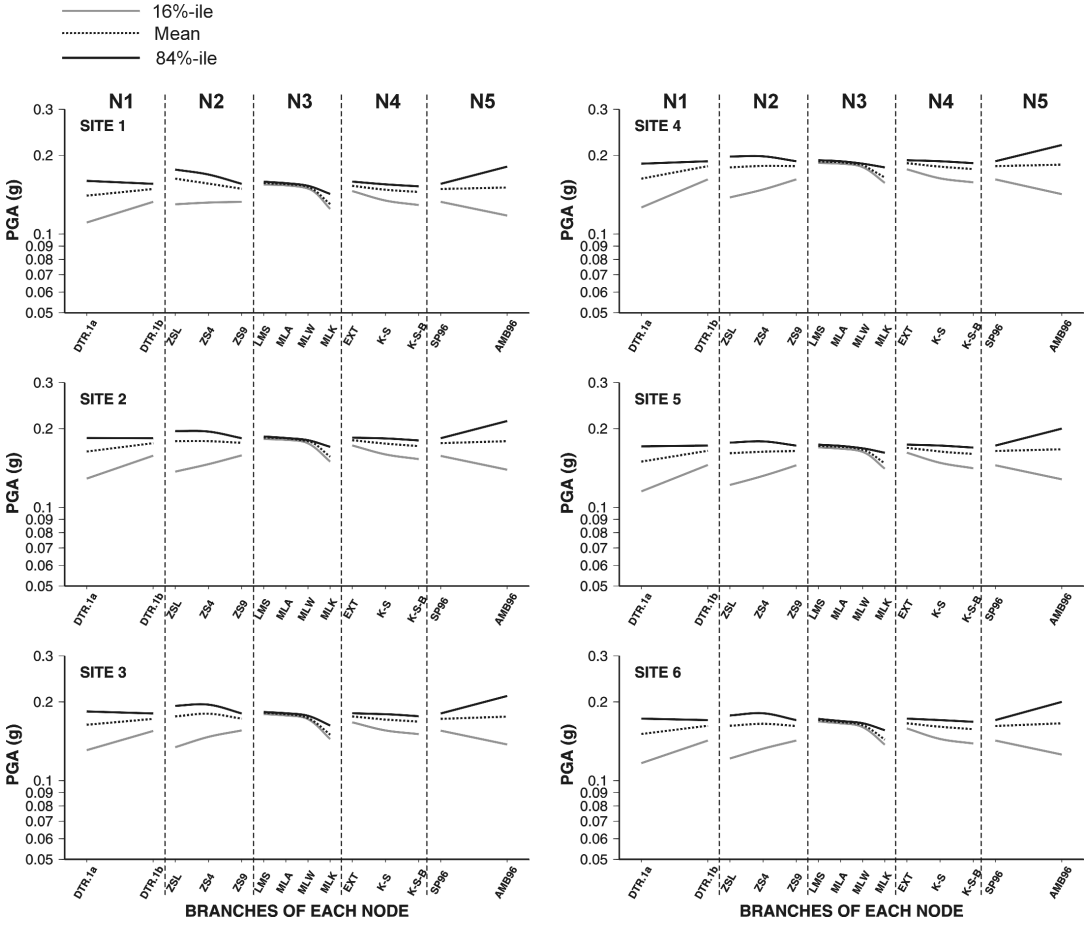


Fig. 9 - PGA values corresponding to a MRP of 475 years for each branch of the preliminary logic tree at each site. Each parameter is allotted the same plotting width.

expected ground motion value that corresponds to a given annual exceedance rate (or, conversely, in the annual rate of exceedance of a given ground motion level) produced by considering all the branch options at that node.

The sensitivity analysis is conducted for all the parameters included in the preliminary logic tree shown in Fig. 1 and it is performed for six test sites (Fig. 7), three along the coast and three inland, located along the expected path of decreasing seismic activity and close to locations of highly felt intensity during past earthquakes. For each site, the ground motion is assessed in terms of the mean horizontal PGA with a 10% probability of exceedance in 50 years using the standard approach established by Cornell (1968). Besides the expected value of the true, but unknown, horizontal PGA that is exceeded, on average, once every 475 years, we also compute the 16$^{th}$ percentile and 84$^{th}$ percentile estimates of that quantity.

The exceedance probability of particular PGA values is computed using a computer program developed at the University of Genoa, which is based on the PSHA software by Dr. Norman

Abrahamson. The program, called HAZ_MULTI, is developed in C language. Basic input data are: geometry of each source zone (longitude and latitude of each polygon vertex), depth, prevalent mechanism of faulting, frequency-magnitude parameter ($\upsilon$, $b$) values, minimum and maximum magnitude values of all the sources. The set of the most common European attenuation relationships (e.g. Ambraseys *et al*., 1996; Sabetta and Pugliese, 1996) is provided by the software. The hazard code computes hazard curves for a single site or for a grid of points, and ground motions for specific return periods. The seismicity of the sources is modelled as a Poisson process. The mean annual rate of exceedance of a ground motion parameter value $y^*$ is computed as:

$$\lambda_{y^*} = \sum_{i=1}^{N_S} \upsilon_i \iiint P\left[Y > y^* \mid m,r,\varepsilon\right] f_{\mathrm{M,R}}\left(m,r\right) f_{\varepsilon}\left(\varepsilon\right) dm\ dr\ d\varepsilon \tag{8}$$

where $\upsilon_i$ [= exp( $\alpha_i$- $\beta_i$ $m_0$)] is the average rate of threshold magnitude exceedance for each one of the $N_S$ potential earthquake sources, $P[Y > y^* \mid m, r, \varepsilon]$ is the probability that a particular ground motion parameter $Y$ exceeds a certain value, $y^*$, for an earthquake of a given magnitude, $m$, occurring at a given distance, $r$, and number of standard deviations of the ground motion (above the median ground motion), $\varepsilon$, $f_{\mathrm{M,R}}(m, r)$ is the joint probability density function of magnitude and distance, and $f_{\varepsilon}(\varepsilon)$ is the probability density function for the ground motion variability. The ground motion distribution is truncated at $\varepsilon = 3$ standard deviations.

For each seismogenic source, the logic tree approach generates a large number of alternative branches for the computation of the hazard at a site. The hazard at a site, as shown in the equation above, is computed by adding the contribution from each source. Each hazard curve is produced by independently sampling the hazard contribution of each source. The probability that a branch associated with a particular source is selected in the simulation is equal to the weight associated to each branch. The only constraint enforced on the sampling procedure is the choice of the attenuation model that in each simulation, once sampled for the first source, is kept constant for all the sources.

In order to analyse the sensitivity of each parameter of the preliminary logic tree (Fig. 1), the influence of each node and its branches on the seismic hazard results needs to be identified (Giner *et al*., 2002a). In this study, we evaluate the effect of each parameter on mean values of PGA corresponding to a MRP of 475 years, the 16$^{th}$ percentile, and the 84$^{th}$ percentile. For example, suppose one wants to evaluate the sensitivity of Node N1 (Fig. 1) at Site 1. This node has two branches that represent two different catalogues. Therefore, we have to evaluate the contribution to the hazard from DTR.1a and DTR.1b. First, the mean hazard curve for PGA values and the hazard curves corresponding to the 16$^{th}$ percentile and 84$^{th}$ percentile are determined accounting for all the logic tree solutions obtained by using DTR.1a (Fig. 8a). Then we calculate the hazard curves accounting for the combination of models and parameters associated with Branch DTR.1b (Fig. 8a). Subsequently, we plot the PGA values corresponding to a MRP of 475 years against the labels of the two alternative branches (Fig. 8b) on a log-scale. The use of a log-scale is employed since hazard results and their uncertainties are generally modelled by a lognormal distribution (Reiter, 1991). The branch labels are represented by using

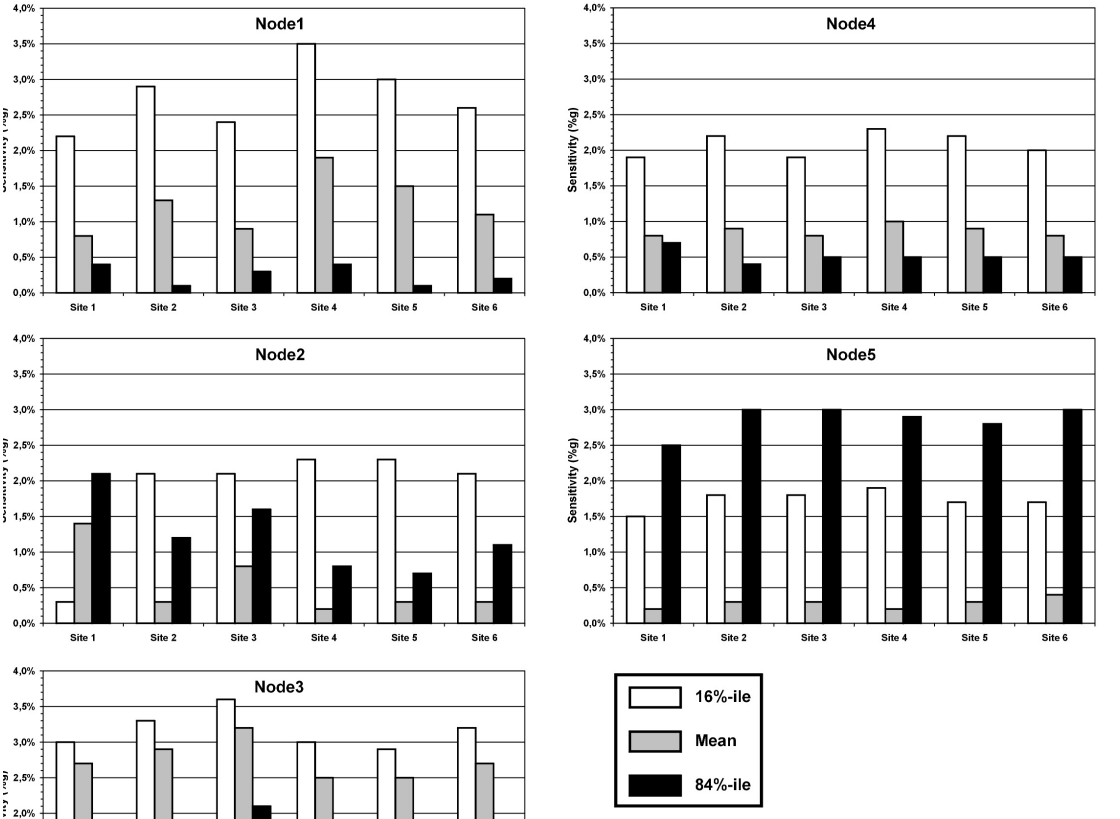


Fig. 10 - Sensitivity of each node of the logic tree at each site. The influence on mean values of PGA (%g), the 16$^{th}$ percentile and the 84$^{th}$ percentile is shown.

a variable that takes values -1 for Branch DTR.1a and +1 for Branch DTR.1b. The sensitivity of the node is quantified by the range in the PGA values with a 10% probability of exceedance in 50 years produced by considering the two catalogues. If the node has a little impact on the hazard, the difference between the PGA values should be nearly equal to zero [according to Giner *et al*. (2002a), the sensitivity is considered negligible if ≤ 1% g], otherwise the ground motion should vary quite a lot. Node N1 has a moderate influence on the 16%-ile since the sensitivity is about 2.2% g. The effects on mean PGA values and the 84%-ile are negligible. Besides the range in the PGA values, a measure of the sensitivity of a node is also provided by the first order coefficient of a regression analysis performed on the PGA values estimated for each branch of a node (regression is not necessary in the aforementioned example since Node N1 has two branches, Fig. 8b) (Rabinowitz *et al*., 1998; Giner *et al*., 2002b).

Following the same procedure, we evaluate the sensitivity of each parameter of the

preliminary logic tree (Fig. 1) at each one of the six considered sites. As a result, the sensitivity analysis allows us to identify the parameters that have the largest impact on the hazard and contribute most to its uncertainty.

## 6. Results and discussion

The influence of each branch of the preliminary logic tree on the assessed hazard is shown in Fig. 9 where the PGA values for a MRP of 475 years are plotted on a log-scale for each global alternative. A positive slope of the curves (ascending curves) indicates an increment of the PGA values from one branch to another of a node (e.g. the DTR.1b catalogue has a positive effect on the hazard since it increases the values of PGA). On the contrary, descending curves represent a decrement of the PGA values (e.g. branch MKL has a negative effect since it decreases the hazard). The higher the slope of the curves, the more the increment/decrement of the PGA values is and, consequently, the sensitivity. Furthermore, Fig. 9 allows us to quantify the contribution of each branch of a node to the uncertainty in the hazard through the differences between the 84 percentile and the 16 percentile. As the spread of the two percentiles increases, the contribution to the uncertainty also increases. Fig. 10 summarizes the results shown in Fig. 9 by plotting the sensitivity (range in the PGA values corresponding to a MRP of 475 years) of each node for the six test-localities.

**Node N1 (seismic catalogues)** has the highest effect on mean PGA values and the 16 percentile at Site 4 since the sensitivity is up to 1.9% g and 3.5% g respectively (Fig. 10). Nevertheless, the node does not show substantial regional variations of the sensitivity that are, on average, a little higher inland (Site 4, 5 and 6) than along the coast (Site 1, 2 and 3). The effect of this node on the $84^{th}$ percentile is negligible (≤ 1%g) at all the sites. Fig. 9 shows that the catalogue DTR.1a always provides the lowest hazard and the largest differences between the $84^{th}$ percentile and the $16^{th}$ percentile (up to 5.9% g at Site 4).

Except for Site 1, **Node N2 (source zone models)** has a moderate influence on the $16^{th}$ percentile (Fig. 10). The effect on mean PGA values is negligible at all the sites with the exception of Site 1 where the sensitivity is equal to 1.4% g. The influence on the $84^{th}$ percentile is a little higher along the coast (Site 1, 2 and 3) than inland (Site 4, 5 and 6) where it is negligible. The smallest contribution to the uncertainty in the hazard from the ZS9 model (Fig. 9) may be explained by the size of the source zones that are larger than those of ZS4 and ZSL.

Fig. 9 shows that the different procedures used to calculate the frequency-magnitude parameters (**Node N3**) have a moderate impact on the hazard. The only procedure giving different results, and consequently a high sensitivity, is the one from Kijko and Sellevoll (MLK) because it also affects the completeness. In fact, the values of the parameters ($\upsilon$, $b$) obtained by using the Kijko and Sellevoll procedure (MLK) always provide the lowest PGA values and the largest differences between the $84^{th}$ percentile and the $16^{th}$ percentile (Fig. 9). The largest contribution to the uncertainty from this approach may be explained by the use of incomplete historical data (from year 1000) for the computation of the recurrence parameters. LMS, MLA and MLW contribute about the same amount to the overall hazard. As shown in Fig. 10, the sensitivity decreases slightly from the coast to the hinterland where it reaches its minimum values at Site 5. The highest influence is observed at Site 3 for both mean PGA values and the two percentiles

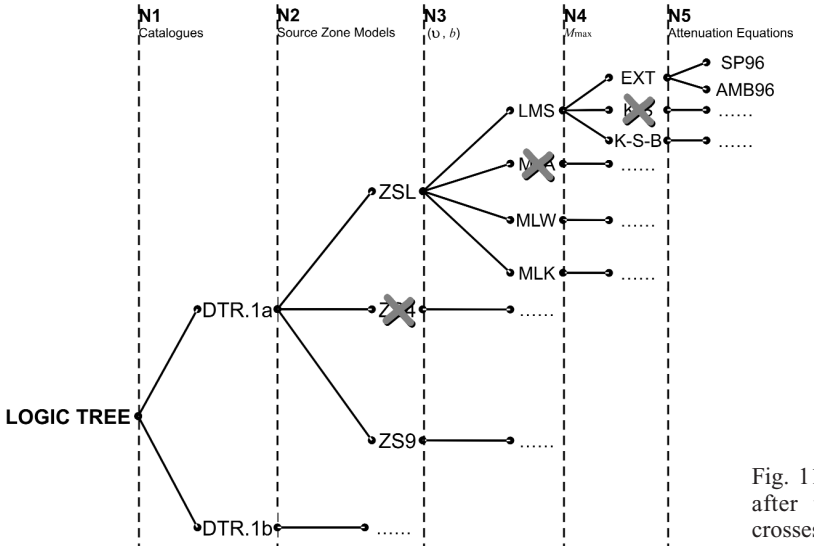


Fig. 11 - "Pruned" logic tree obtained after the sensitivity analysis. Grey crosses indicate the "pruned" branches.

considered.

**Node N4 (maximum earthquake magnitude)** has a negligible effect on both mean PGA values and the 84$^{th}$ percentile. The influence on the 16$^{th}$ percentile varies from 1.9% g at Site 1 to 2.3% g at Site 4 (Fig. 10). Fig. 9 shows that the values of $M_{max}$ calculated by the application of the EXT procedure always provide the highest hazard, whereas those computed by using K-S-B give the lowest PGA values at all the sites and contribute most to the uncertainty (the difference between the 84$^{th}$ percentile and the 16$^{th}$ percentile reaches its maximum at Site 6 where it is equal to 2.9% g).

**Node N5 (attenuation models)** has a great effect on the 84 percentile since the sensitivity varies from 2.5% g to 3.0% g. The influence on mean values of the PGA is negligible while a moderate impact on the 16$^{th}$ percentile may be observed (Fig. 10). Moreover, AMB96 contributes most to the variability in the hazard (Fig. 9): in fact, the difference between the 84$^{th}$ percentile and the 16$^{th}$ percentile goes up to 7.7% g. The smallest contribution to the uncertainty in the hazard from SP96 may be explained by the use of Italian data to derive the equation.

The results just described show that the influence of the considered nodes on the hazard is independent of the study site since regional variations of the sensitivity are modest (sensitivities vary modestly from site to site). Also the variations of the absolute PGA values among the sites considered are modest (they reach 2% g maximum). Values of PGA are generally higher along the coast than inland (compare, for example, Site 2 and Site 5 or Site 3 and site 6 in Fig. 9), in agreement with the distribution of the macroseismic intensities (see Fig. 3) which decrease from coast to inland.

Following the previous results, we can "prune" the branches with little effect on the hazard from the logic tree shown in Fig. 1. These branches can be neglected in future logic tree analyses. Further research on them is a waste of time and money. Branches with little influence are "pruned" from the preliminary logic tree by applying simple rules that were established by

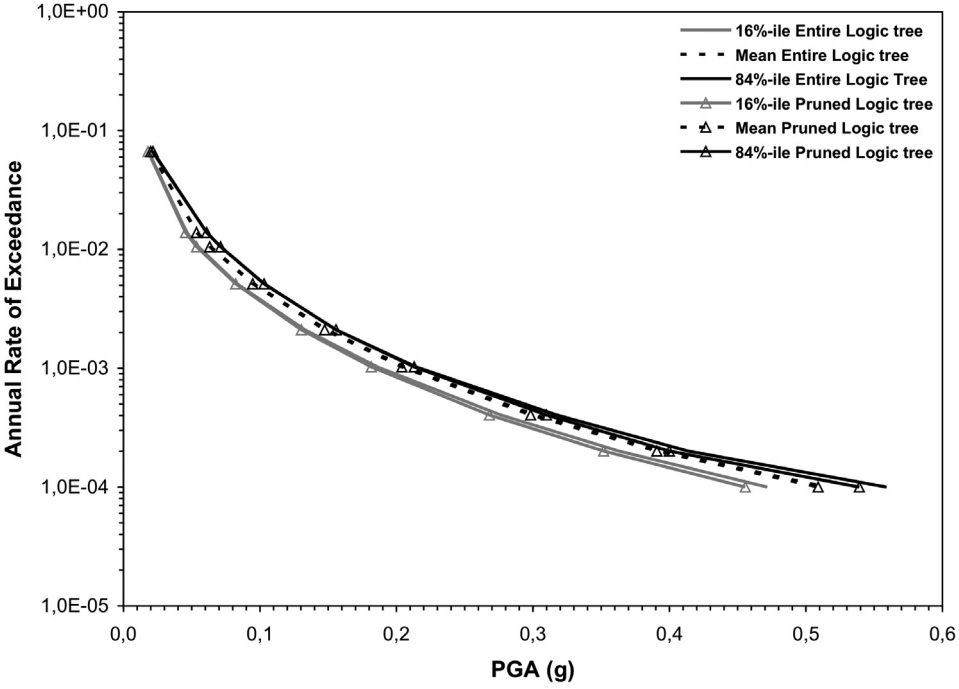


Fig. 12 - Comparison between the seismic hazard curves for PGA resulting from the application of the preliminary and the "pruned" logic trees. Hazard curves refer to Site 1.

Rabinowitz *et al*. (1998) and are adapted here to consider the effect on both mean PGA values and the two percentiles considered:

1. only one branch is kept if a node has little or no effect (range in the PGA values ≤1% g) on mean values of PGA, the $16^{th}$ percentile, and the $84^{th}$ percentile;
2. two branches can be considered if a node with high sensitivity has a linear effect (see, for example, Node N1 in Fig. 9);
3. if a node exhibits some curvature (see, for example, Node N3 in Fig. 9), then all the branches of that node must be considered in the "pruned" logic tree.

Following these rules, no "pruning" is possible from the nodes with two branches. For the remaining nodes, Fig. 9 shows that linear effects prevail. Only Node N3 presents substantial quadratic effects. However, since this node exhibits a linear tendency in the intervals LMS-MLW, one branch can be "pruned" as stated by rule 2). The extreme branches of the above mentioned interval are included in the "pruned" logic tree while Branch MLA is "pruned". Other modest quadratic effects can be observed at Node N2 and N4 (Fig. 9), but they are neglected; therefore, ZS4 and KS branches can be "pruned" and the extreme branches are kept. Fig. 11 shows the "pruned" logic tree. It consists of 48 terminal branches (instead of the preliminary 144) that represent the parameters that contribute most to the overall hazard associated to western Liguria. Future research on these parameters will reduce the uncertainty in the hazard and yield better hazard estimates. To verify the conclusion that the "pruned" branches are superfluous (since they have little or no effect on the hazard), we repeat the hazard calculations by using the "pruned"

logic tree and compare the mean, 16$^{th}$ percentile and 84$^{th}$ percentile hazard curves for PGA with those obtained from the preliminary logic tree (Fig. 12). If the "pruned" branches are really superfluous, then the "pruned" logic tree should provide the same results as the preliminary logic tree without any reduction of the uncertainty. Fig. 12 clearly shows an overlap of the corresponding curves calculated at Site 1 (analogous results have been obtained for the other sites and are not presented here) and demonstrates the correctness of our results.

## 7. Conclusions and remarks

The sensitivity analysis, as suggested by Rabinowitz and Steinberg (1991), provides a useful feedback loop for an intelligent construction of logic trees since it allows one to get parameters into insight. In this study, a multi-parameter sensitivity analysis has been conducted in order to quantify the influence of different parameters on the western Ligurian seismic hazard. Both the effect of each node and its branches on mean values of PGA corresponding to a MRP of 475 years and their influence on two different percentiles (16$^{th}$ percentile and 84$^{th}$ percentile) are defined. However, the sensitivity analysis can easily be extended to consider other percentiles and spectral acceleration values. Sensitivity studies accounting for spectral acceleration values instead of PGA might be useful to analyze the influence of different attenuation relationships on the hazard in depth. In fact, lower frequencies of ground motion (e.g. spectral accelerations at 1-2 seconds) should emphasize the effect of alternative attenuation relationships.

It has been discovered that the nodes of the preliminary logic tree corresponding to the seismic catalogues (Node N1) and the frequency-magnitude parameters (Node N3) have the highest influence on mean PGA values and the 16$^{th}$ percentile while the attenuation relationships (Node N5) have the highest effect on the 84$^{th}$ percentile. However, it is worth noting that the high sensitivity of Node N3 is mainly due to the Kijko and Sellevoll procedure (MLK) since it has allowed us to account for incomplete historical data for the computation of the recurrence parameters. Furthermore, we found that the DTR.1a catalogue (it includes the offshore localizations of the 1818, 1819, 1854 and 1887 earthquakes), the seismogenetic zonations characterized by smaller source zones, ZS4 and ZSL, and the Ambraseys *et al*. (1996) attenuation equation contribute most to the uncertainty in the hazard. However, these results might be considered valid just for a medium-low seismicity and a short historical information area such as western Liguria, and for a similar set of assumptions. They cannot be extrapolated to different Italian regions characterized by higher seismicity where previous studies (e.g. Lucantoni *et al*., 2001) show much higher sensitivity to the variation of a single parameter.

As a result, the sensitivity analysis has provided useful information for the construction of a future logic tree for probabilistic seismic hazard analysis of western Liguria. The knowledge of the parameters with the largest effect on the hazard is an invaluable guide to determine directions of research that will reduce the uncertainties in the hazard associated with this region. The parameters with little or no effect can be excluded from subsequent logic tree studies.

**Acknowledgements.** We are grateful to Dr. A. Akinci and an anonymous reviewer for their critical review, suggestions, and helpful comments. We are also very thankful to Dr. A. Kijko who provided the software

to compute seismicity parameters. Special thanks are due to the RSNI staff.

## REFERENCES

Aki K.; 1965: *Maximum likelihood estimate of b in the formula Log N = a – bM and its confidence limits*. Bull. Earth. Res. Inst, **43**, 237-239.

Ambraseys N.N., Simpson K.A. and Bommer J.J.; 1996: *Prediction of horizontal response spectra in Europe.* Earthquake Engineering and Structural Dynamics, **25**, 371-400.

Atkinson G.M. and Charlwood R.G.; 1983: *Uncertainties in probabilistic seismic hazard assessment as a function of probability level: a case history for Vancouver, British Columbia*. Bull. Seis. Soc. Am., **73**, 1225-1241.

Augliera P., Béthoux N., Déverchère J. and Eva E.; 1994: *The Ligurian Sea; New seismotectonic evidence.* Boll. Geofis. Teor. Appl., **36**, 363-380.

Augliera P., Cattaneo M., Coppari H., Di Giovanbattista R., Durì G., Frapiccini M., Gasperini P., Gervasi A., Govoni A., Guerra I., Marchetti A., Marsan P., Milana G., Monachesi G., Moretti A., Moroncelli L., Orlanducci L., Parolai S., Renner G., Spallarossa D., Trojani L. and Vannucci G.; 1998: *Catalogo strumentale dei terremoti dal 1981 al 1996.* http://gndt.ingv.it/Pubblicazioni/CDROM/Gasperini/CD_ROM_Gasperini_Leggimi.htm.

Bender K.B. and Perkins D.M.; 1993: *Treatment of parameter uncertainty and variability for a single seismic hazard map.* Earthq. Spectra, **9**, 165-195.

Béthoux N., Frechet J., Guyoton F., Thouvenot F., Cattaneo M., Eva C., Nicolas M. and Granet M.; 1992: *A closing Ligurian Sea?*. Pageoph., **139**, 179-194.

Bommer J.J., Douglas J. and Strasser F.O.; 2003: *Style-of-faulting in ground motion prediction equations.* Bull. Earth. Eng., **1**, 171-203.

Bommer J.J., Scherbaum F., Bungum H., Cotton F., Sabetta F., Abrahamson N.A.; 2005: *On the use of logic trees for ground-motion prediction equations in seismic hazard analysis.* Bull. Seis. Soc. Am., **95**, 377-389.

Cao T., Petersen M. D. and Frankel A. D.; 2005: *Model uncertainties of the 2002 update of California seismic hazard maps*. Bull. Seis. Soc. Am., **6**, 2040-2057.

Chaumillon E., Deverchere J., Rehault J.P., Gueguen E.; 1994: *Réactivation tectonique et flexure de la merge continentale ligure (Méditerranée Occidentale)*. C.R. Acad. Sci. Paris, **319**, 675-682.

Contrucci I., Nercessian A., Béthoux N., Mauffret A., Pascal G.; 2001: *A Ligurian (Western Mediterranean Sea) geophysical transect revisited*. Geophys. J. Int., **146**, 74-97.

Cornell C. A.; 1968: *Engineering seismic risk analysis.* Bull. Seis. Soc. Am., **58**, 1583-1606.

Cramer C.H., Petersen M.D. and Reichle M.S.; 1996: *A Monte Carlo approach in estimating uncertainty for a seismic hazard assessment of Los Angeles, Ventura, and Orange Counties, California*. Bull. Seis. Soc. Am., **86**, 1681-1691.

Eva C. and Rabinovich A. B.; 1997: *The February 23, 1887 tsunami recorded on the Ligurian coast, western Mediterranean*. Geophys. Res. Lett., **24**, 2211-2214.

Eva C., Augliera P., Eva E., Solarino S. and Spallarossa D.; 2000: *Sintesi delle conoscenze sulla sismotettonica della Liguria occidentale ed influenza sui parametri di hazard.* In: Galadini F., Meletti C. and Rebez A. (ed), Le ricerche del GNDT nel campo della pericolosità sismica (1996-1999), CNR - Gruppo Naz. Difesa Terremoti, Roma, pp. 59-70.

Eva E. and Solarino S.; 1998: *Variations of stress directions in the western Alpine arc*. Geophys. J. Int., **135**, 438-448.

Eva E., Solarino S. and Spallarossa D.; 2001: *Seismicity and crustal structure beneath the western Ligurian Sea derived from local earthquake tomography.* Tectonophysics, **339**, 495-510.

Ferrari G.; 1991: *The 1887 Ligurian earthquake: a detailed study from contemporary scientific observations*. Tectonophysics, **193**, 131-139.

Giner J.J., Molina S. and Jauregui P.; 2002a: *Advantages of using sensitivity analysis in seismic hazard assessment: a case study of sites in southern and eastern Spain*. Bull. Seism. Soc. Am., **92**, 543-554.

Giner J.J., Molina S., Jauregui P. and Delgado J.; 2002b: *A new methodology for decreasing uncertainties in the seismic hazard assessment results by using sensitivity analysis. An application to sites in Eastern Spain*. Pure appl. Geophys., **159**, 1271-1288.

Grandori G., Drei A., Perotti F. and Tagliani A.; 1991: *Macroseismic intensity versus epicentral distance: the case of Central Italy.* Tectonophysics, **193**, 165-171.

Grünthal G. and Wahlström R.; 2001: *Sensitivity of parameters for probabilistic seismic hazard analysis using a logic*

*tree approach*. Jour. Earth. Eng., **5,** 309-328.

Gruppo di lavoro CPTI; 2004: *Catalogo Parametrico dei Terremoti Italiani, versione 2004 (CPTI04)*. INGV, Bologna. http://emidius.mi.ingv.it/CPTI/.

Gruppo di lavoro MPS; 2004a: *Redazione della mappa di pericolosità sismica prevista dall'Ordinanza PCM del 20 marzo 2003. Rapporto conclusivo per il dipartimento di Protezione Civile, INGV, Milano – Roma, aprile 2004, 65 pp. + 5 appendici. The website has been changed to: http://zonesismiche.mi.ingv.it/elaborazioni/.*

Gruppo di lavoro MPS; 2004b: *Appendice 1 al Rapporto Conclusivo – Catalogo dei terremoti CPTI2. The website has been changed to: http://zonesismiche.mi.ingv.it/elaborazioni/.*

Gruppo di lavoro MPS; 2004c: *Appendice 2 al Rapporto Conclusivo – Zonazione sismogenetica ZS9. The website has been changed to: http://zonesismiche.mi.ingv.it/elaborazioni/.*

Kijko A.; 2004: *Estimation of the maximum earthquake magnitude,* $m_{max}$. Pure Appl. Geophys., **161**, 1-27.

Kijko A. and Graham G.; 1998: *Parametric-historic procedure for probabilistic seismic hazard analysis. Part I: estimation of maximum regional magnitude* $m_{max}$. Pure Appl. Geophys., **152**, 413-442.

Kijko A. and Sellevoll M.A.; 1989: *Estimation of earthquake hazard parameters from incomplete data files. Part I. Utilization of extreme and complete catalogues with different threshold magnitudes.* Bull. Seis. Soc. Am., **79**, 645-654.

Kijko A. and Sellevoll M.A.; 1992: *Estimation of earthquake hazard parameters from incomplete data files. Part II. Incorporation of magnitude heterogeneity.* Bull. Seis. Soc. Am., **82**, 120-134.

Kramer S.L.; 1996: *Geotechnical earthquake engineering*. Prentice-Hall, New Jersey, pp. 106-139.

Kulkarni R.B., Youngs R.R. and Coppersmith K.J.; 1984: *Assessment of confidence intervals for results of seismic hazard analysis.* In: Proceedings of the Eighth World Conference on Earthquake Engineering, San Francisco, vol. 1, pp. 263-270.

Lucantoni A., Bosi V., Bramerini F., De Marco R., Lo Presti T., Naso G. and Sabetta F.; 2001: *Il rischio sismico in Italia.* Ingegneria Sismica, Anno XVIII, **1**, 5-37.

McGuire R.K and Arabasz W.S.; 1990: *An introduction to probabilistic seismic hazard analysis*. In: Ward S.H. (ed), Geotechnical and Environmental Geophysics, Cambridge University press, Cambridge, 1, pp. 333-352.

McGuire R.K. and Shedlock K.M.; 1981: *Statistical uncertainties in seismic hazard evaluations in the United States.* Bull. Seis. Soc. Am., **71**, 1287-1308.

Meletti C., Patacca E. and Scandone P.; 2000: *Construction of a seismotectonic model: the case of Italy*. Pure Appl. Geophys., 157, 11-35.

Monachesi G. and Stucchi M.; 2000: *DOM4.1 un database di osservazioni macrosismiche di terremoti di area italiana al di sopra della soglia del danno.* http://emidius.mi.ingv.it/DOM/

Montaldo V., Faccioli E., Zonno G., Akinci A. and Malagnini M.; 2005: *Treatment of ground-motion predictive relationships for the reference seismic hazard map of Italy.* Journal of Seismology, **9**, 295-316.

Pasquale V., Verdoya M. and Chiozzi P.; 1994: *Types of crust beneath the Ligurian Sea.* Terra Nova, **6**, 255-266.

Pasquale V., Verdoya M., Chiozzi P. and Ranalli G.; 1996: *Rheology and seismotectonic regime in the northern central Mediterranean*. Tectonophysics, **270**, 239-257.

Pelinovsky E., Kharif C., Riabov I. and Francius M.; 2001: *Study of tsunami propagation in the Ligurian Sea.* Natural Hazards and Earth System Sciences, **1**, 195-201.

Pelinovsky E., Kharif C., Riabov I. and Francius M.; 2002: *Modelling of tsunami propagation in the vicinity of the French coast of the Mediterranean.* Nat. Haz., **25**, 135-159.

Peruzza L.; 1996: *Attenuating intensities*. Ann. Geof., **39**, pp. 1079-1093.

Petersen M.D., Cramer C.H., Frankel A.D.; 2000: *Monte Carlo uncertainty analysis for the hazard from the Cascadia Subduction Zone in the Pacific Northwest of the United States*. In: 2nd ACES (Apec Cooperation for Earthquake Simulation) Workshop. http://tokyo.rist.or.jp/ACES_WS2/extended_abstract/PDF/

Rabinowitz N. and Steinberg D.M.; 1991: *Seismic hazard sensitivity analysis: a multi-parameter approach.* Bull. Seis. Soc. Am., **81**, 796-817.

Rabinowitz N., Steinberg D. M. and Leonard G.; 1998: *Logic trees, sensitivity analyses, and data reduction in probabilistic seismic hazard assessment.* Earth. Spectra, **14**, 189-201.

Reiter L.; 1991: *Earthquake hazard analysis. Issues and insights*. Columbia University Press, New York, 252 pp.

Sabetta F. and Pugliese A.; 1996: *Estimation of response spectra and simulation of nonstationary earthquake ground motions*. Bull. Seism. Soc. Am., **2**, 337-352.

Sadigh K., Chang C.-Y., Egan J. A., Makdisi F. and Youngs R. R.; 1997: *Attenuation relationships for shallow crustal earthquakes based on California strong motion data.* Seism. Res. Lett., **68**, 180-189.

Senior Seismic Hazards Analysis Committee; 1997: *Recommendations for probabilistic seismic hazard analysis: Guidance on uncertainty and the use of experts.* NUREG/CR6372, Nuclear Regulatory Commission, Washington, 256 pp.

Tinti S., Maramai A. and Graziani L.; 2004: *The new catalogue of Italian tsunamis.* Nat. Haz., **33**, 439-465.

Vannucci G. and Gasperini P.; 2004: *The new release of the database of earthquake mechanisms of the Mediterranean area (EMMA Version 2)*. Ann. Geof., supplement to Vol. 47, 307-334.

Vannucci G., Pondrelli S., Argnani A., Morelli A., Gasperini P. and Boschi E.; 2004: *An atlas of Mediterranean Seismicity*. Ann. Geof., supplement to Vol. **47**, 247-306.

Weichert D.H.; 1980: *Estimation of the earthquake recurrence parameters for unequal observation periods for different magnitudes.* Bull. Seis. Soc. Am., **70**, 1337-1346.

*Corresponding author:* Simone Barani
Dipteris, Università di Genova
Sezione Geofisica
Viale Benedetto XV-5, 16132 Genova, Italy
phone: +39-010-3538098; e-mail: barani@dipteris.unige.it